nature astronomy

SUPPLEMENTARY INFORMATION
https://doi.org/10.1038/s41550-018-0442-z

In the format provided by the authors and unedited.

Discovery of rapid whistlers close to Jupiter implying lightning rates similar to those on Earth

Ivana Kolmašová [1,2]*, Masafumi Imai [3], Ondřej Santolík [1,2], William S. Kurth [3], George B. Hospodarsky [3], Donald A. Gurnett [3], John E. P. Connerney [4] and Scott J. Bolton [5]

[1]Department of Space Physics, Institute of Atmospheric Physics, The Czech Academy of Sciences, Prague, Czechia. [2]Faculty of Mathematics and Physics, Charles University, Prague, Czechia. [3]Department of Physics and Astronomy, University of Iowa, Iowa City, IA, USA. [4]NASA/Goddard Spaceflight Center, Greenbelt, MD, USA. [5]Space Science Department, Southwest Research Institute, San Antonio, TX, USA. *e-mail: iko@ufa.cas.cz

Contents:

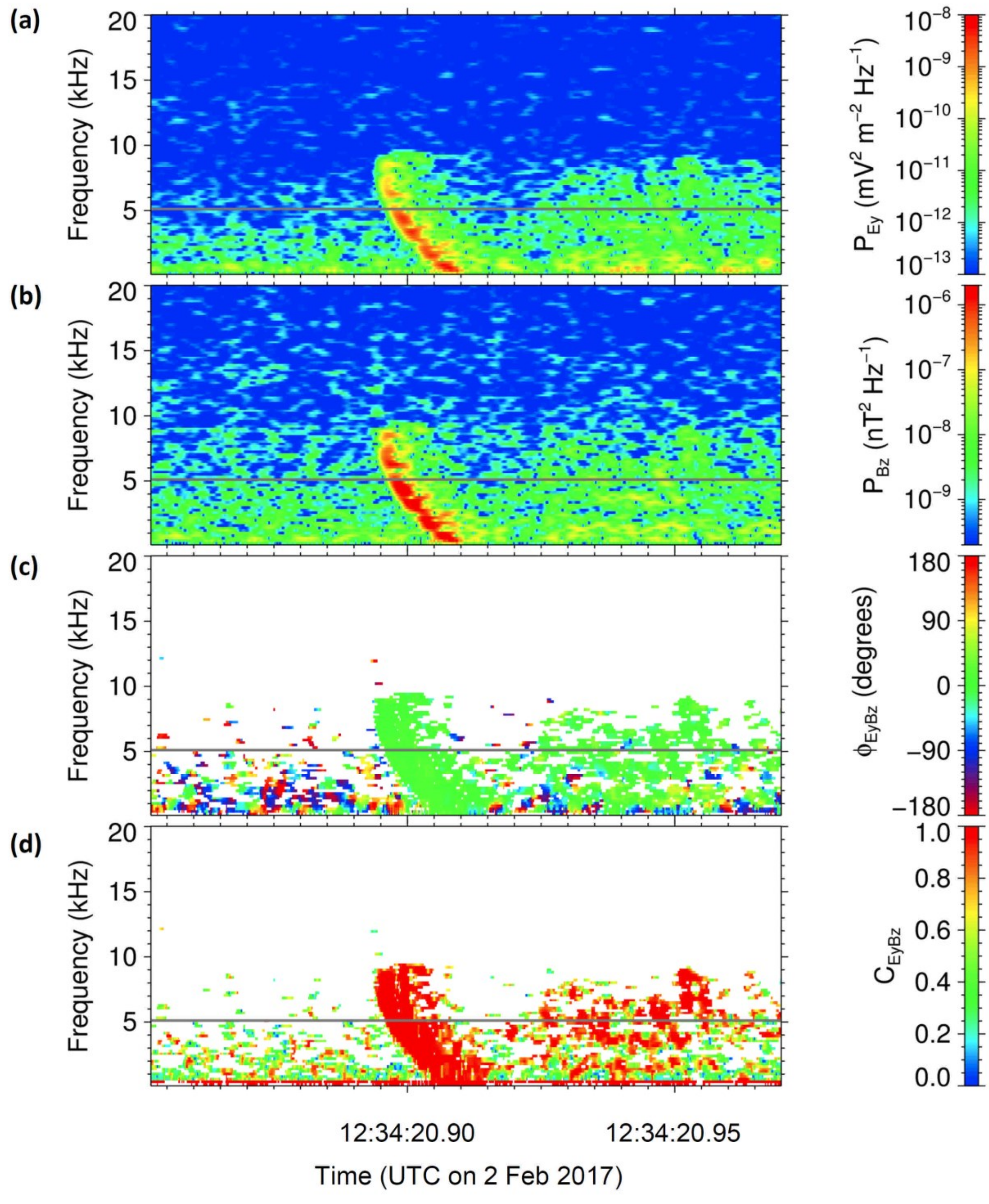

Supplementary Figure 1 | Multicomponent analysis of the waveform record shown in Figure 1a.
(a) frequency-time power spectrogram of the electric field fluctuations (b) power spectrogram of the magnetic field fluctuations (c) frequency-time map of the relative phase $\phi_{E_Y B_Z}$ (Equation 4) between the electric and magnetic field signals (d) frequency-time map of their relative coherency $C_{E_Y B_Z}$ (Equation 3) where values close to unity are obtained for signals without random phase shifts. Horizontal grey line shows the local proton cyclotron frequency (5.11 kHz)

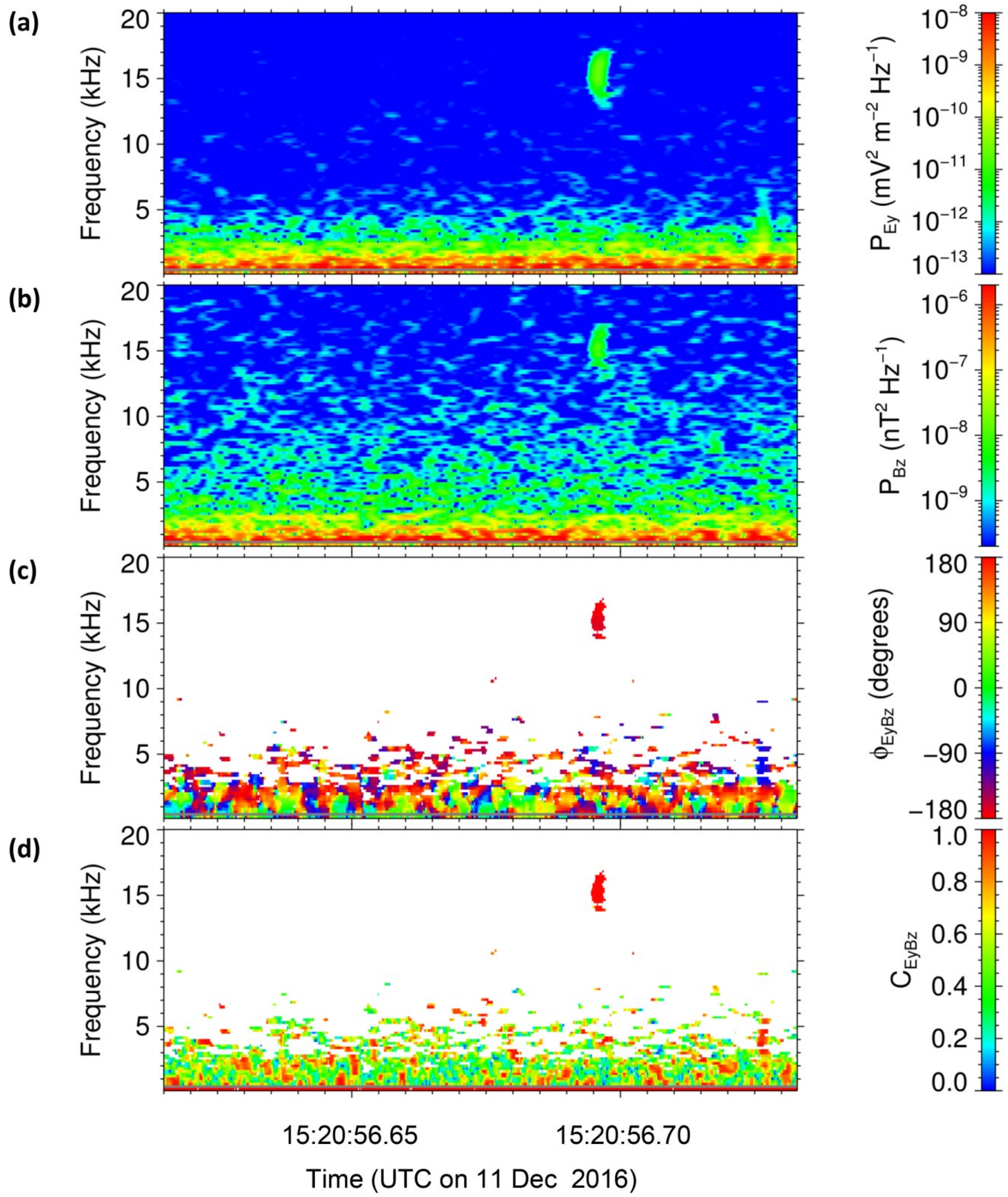

Supplementary Figure 2 | Example of an event which has been excluded from the analysis. The event might be related to lightning but occurs only at frequencies above 10 kHz. The colour scales are given on the right for separate panels: (a) Frequency-time power spectrogram of the electric field fluctuations, (b) power spectrogram of the magnetic field fluctuations, (c) frequency-time map of the relative phase $\phi_{E_Y B_Z}$ (Methods, Equation 4) between the electric and magnetic field signals, and (d) frequency-time map of their relative coherency $C_{E_Y B_Z}$ (Methods, Equation 3) where values close to unity are obtained for signals without random phase shifts.

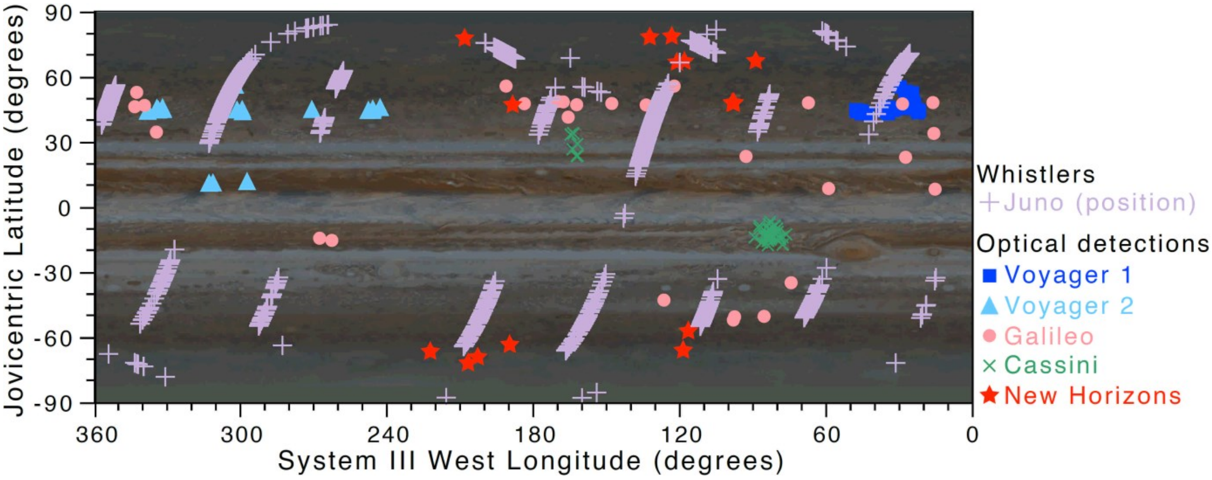

Supplementary Figure 3 | Map of detections of Jovian rapid whistlers as vertical straight line projections of Juno positions down to the planet, compared to previous optical observations. Jovian rapid whistlers are represented by purple '+' symbols; previous measurements are shown according to the legend on the right. The background map was provided by NASA/JPL/Space Science Institute (https://photojournal.jpl.nasa.gov/catalog/PIA07782).

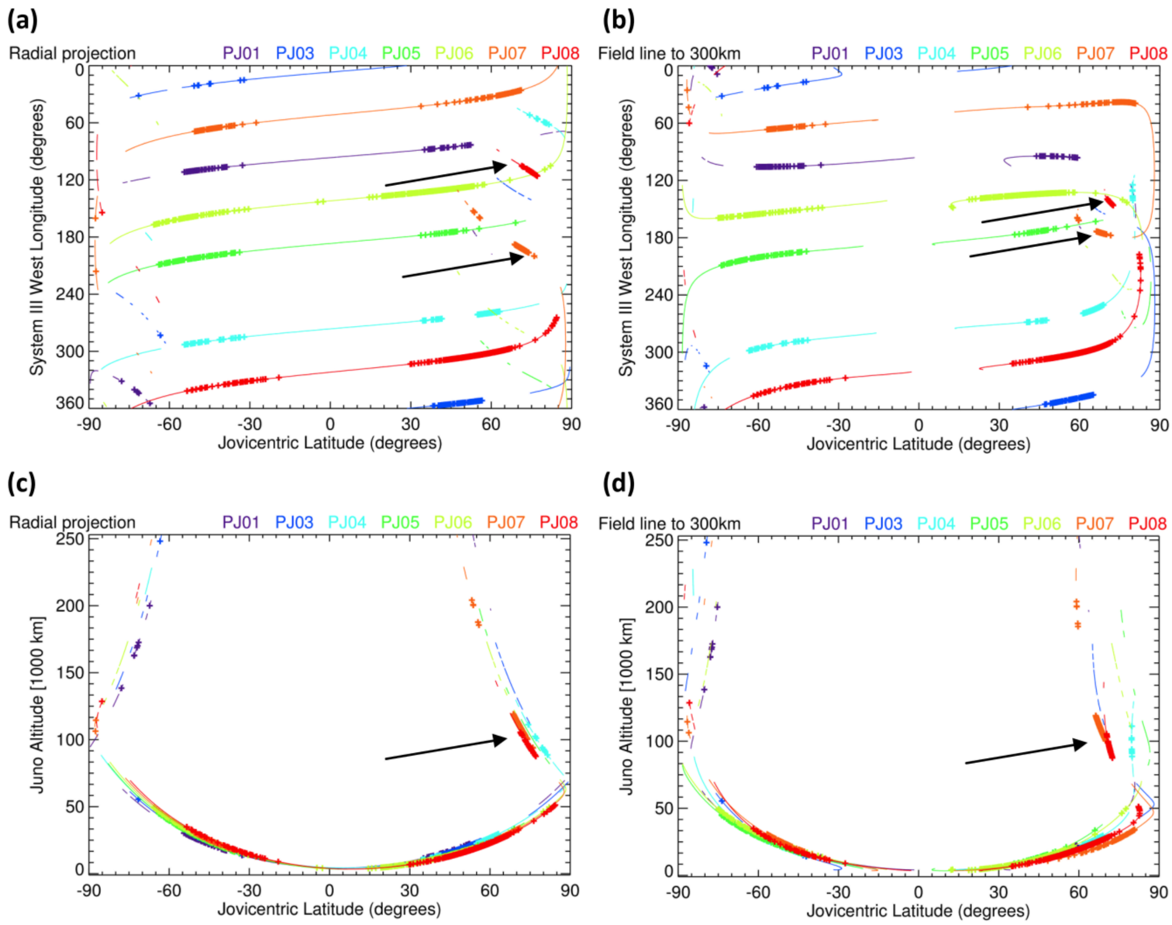

Supplementary Figure 4 | Detections of Jovian rapid whistlers during analysed Juno orbits in a 3D (latitude, longitude, altitude) representation. Separate orbital segments during close approaches to the planet are colour coded according to the legend on the top. Solid lines show Juno positions during continuous burst mode measurements; (a) Vertical projection of Juno position as in Supplementary Fig 3; (b) Magnetic footprint as in Fig. 2; (c) Altitude of measurements versus Juno latitude. (d) Altitude of measurements versus latitude of Juno magnetic footprint. Arrows show the group of detections during the PJ7 and PJ8 orbital segments which contribute to a secondary peak of occurrence as a function of altitude in Fig. 3c.

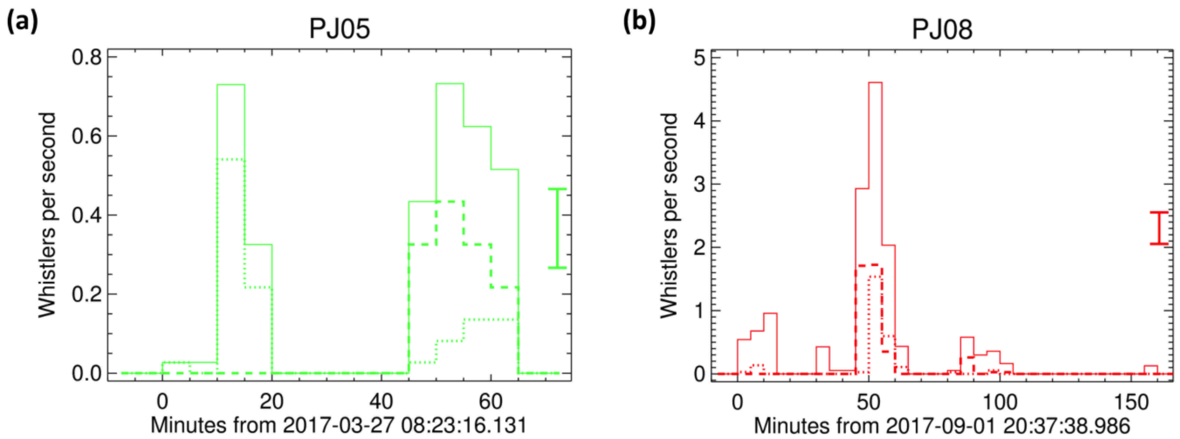

Supplementary Figure 5 | Rates of Jovian rapid whistlers averaged over 5 minute intervals. Number of events per second for (a) the PJ5 orbital segment where we observe the lowest peak rates from our data set and for (b) the PJ8 orbital segment where we observe the highest peak rates from our data set. Solid lines show results for all Jovian rapid whistlers, dotted lines only for dispersion class 1, and dashed lines for dispersion class 2. Error bars for the Poisson statistics are given on the right.

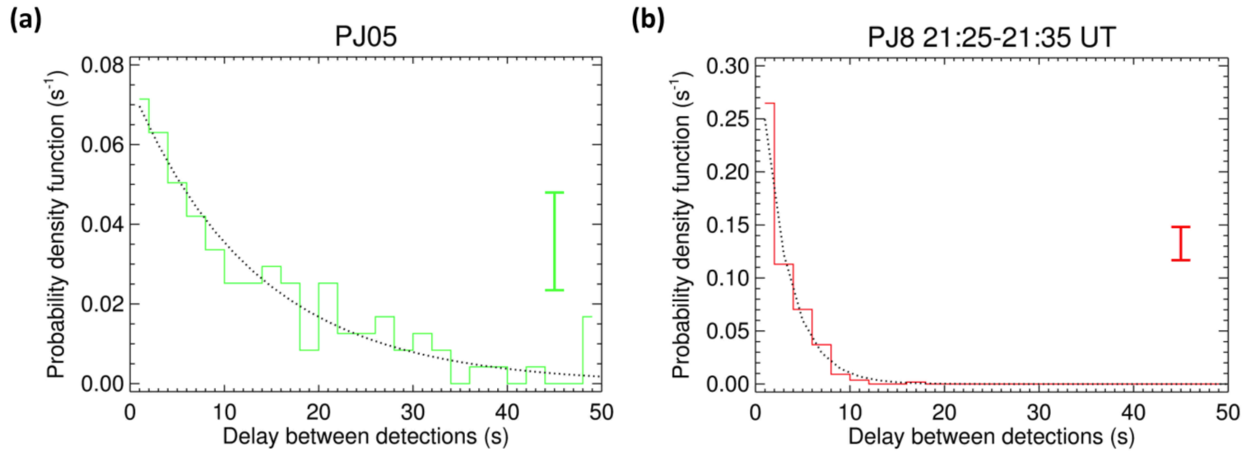

Supplementary Figure 6 | Probability density functions of delays between neighbouring data records which contain detections of Jovian rapid whistlers. Dotted lines show the exponential probability density function of a Poisson random process, $f = \Delta^{-1} \exp(-\tau/\Delta)$, where Δ is the average value of the delay τ between data records for $\tau \leq 50$ s. In the ideal case, the median value of a random variable with this probability distribution should be equal to Δ ln2. Average values of the whistler rates from Supplementary Figure 5 can be obtained from the average delays Δ as K/Δ, where K=1s / 0.12288s=8.14 is the duty cycle coefficient for the burst mode records. (a) Data collected along the PJ5 orbital segment on 27 March 2017 between 8:23 and 9:28 UT, Δ = 13.3 s, median(τ) = 9s ≈ Δ ln2; K/Δ=0.61 events per second. (b) Data collected during the PJ8 orbital segment for the peak rates on 1 September 2017 between 21:25-21:35 UT, Δ = 2.81 s, median(τ) = 2s ≈ Δ ln2, K/Δ=2.9 events per second. Error bars for the Poisson statistics are given on the right.

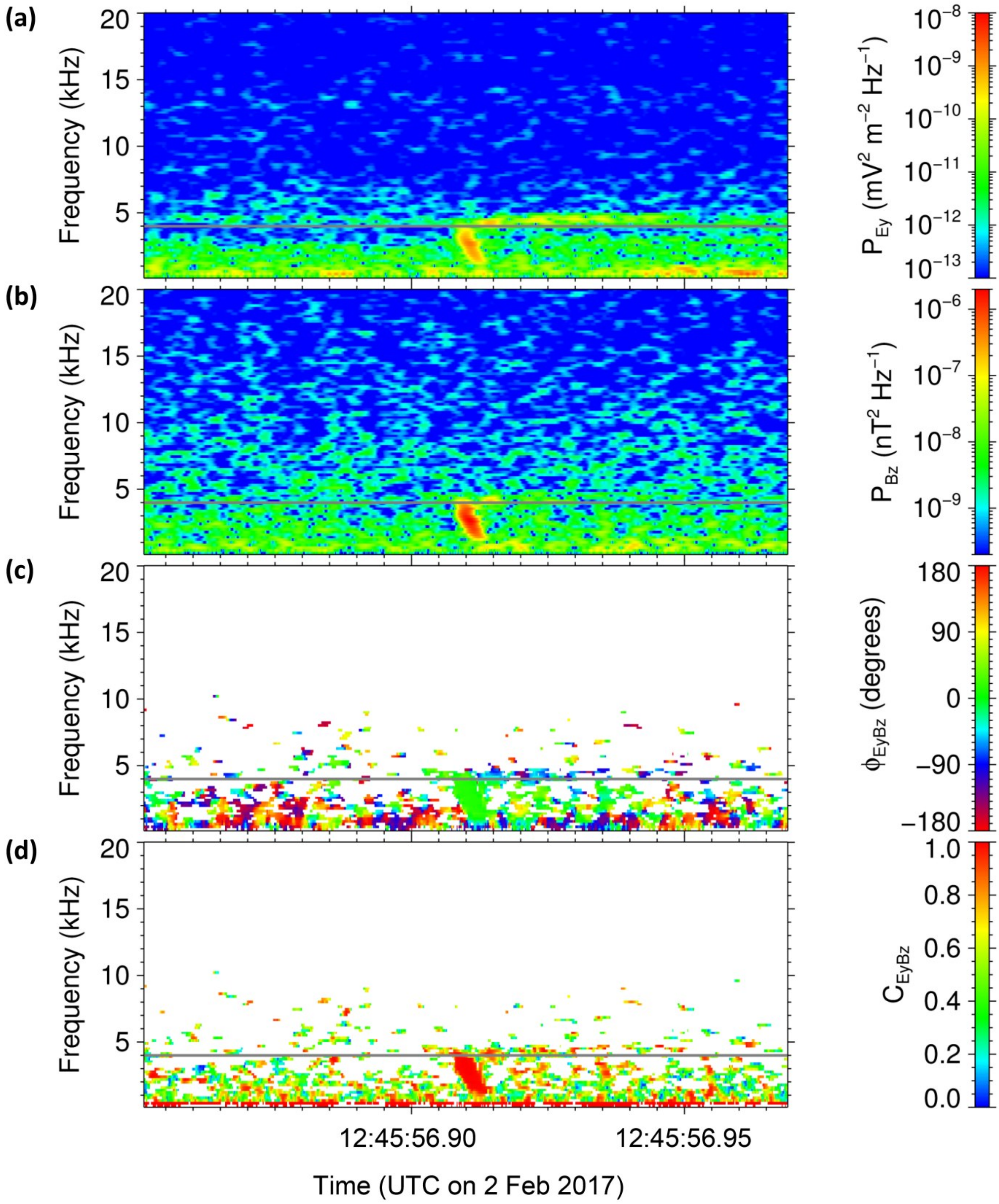

Supplementary Figure 7 | Example of a Jovian rapid whistler for which the dispersion class was not defined. The criterion that frequencies of 2 and 5 kHz are contained within the whistler trace is not met in this case as the signal only extends up to the local proton cyclotron frequency of 3.99 kHz.

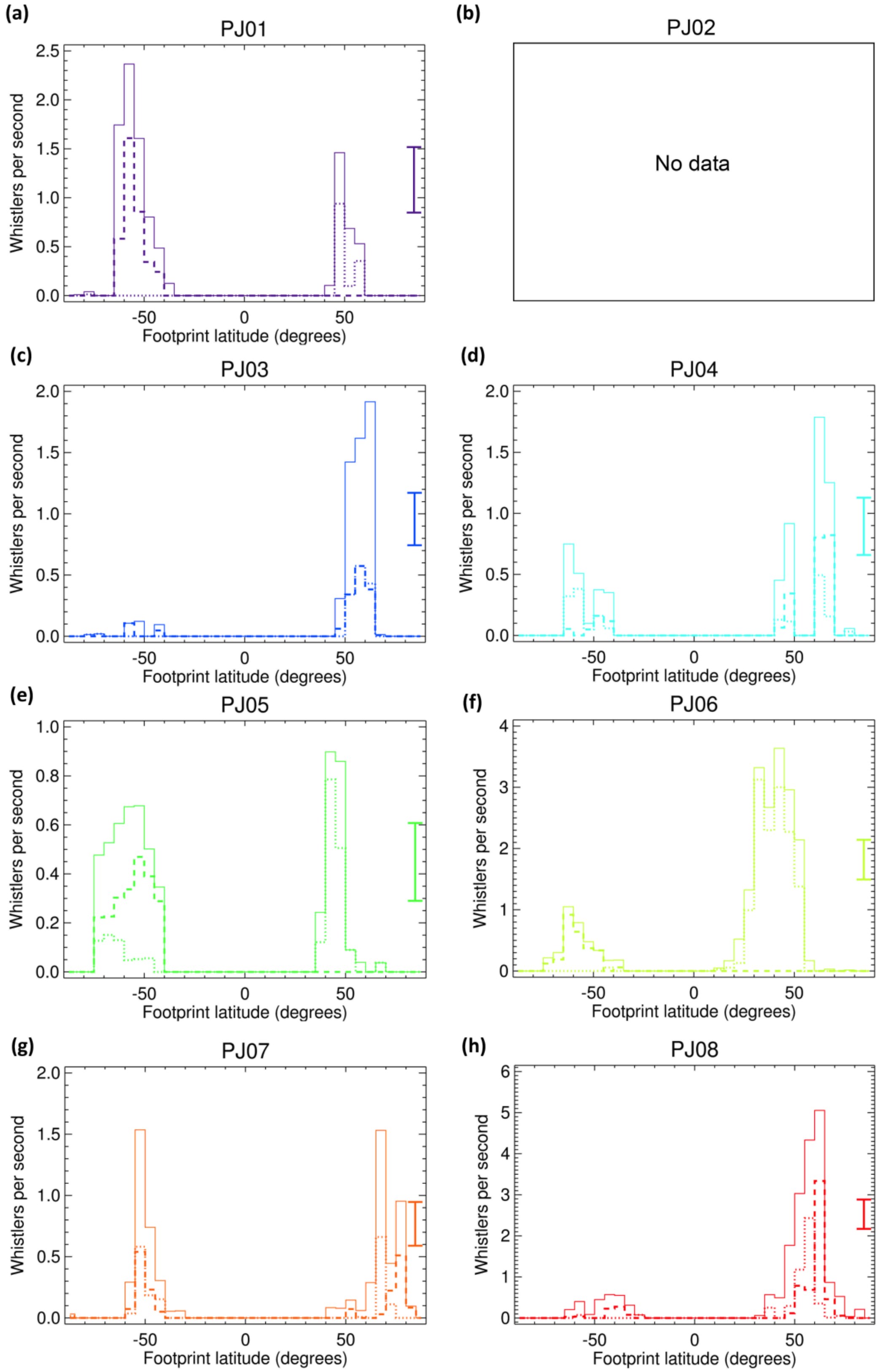

Supplementary Figure 8 | Occurrence rates of Jovian rapid whistlers as a function of the footprint latitude for separate Juno orbits. Dotted, dashed, and solid lines respectively correspond to events with dispersion class 1, to events with dispersion class 2, and to all events, including those for which the class has not been determined. Error bars from Poisson statistics are given on the right.

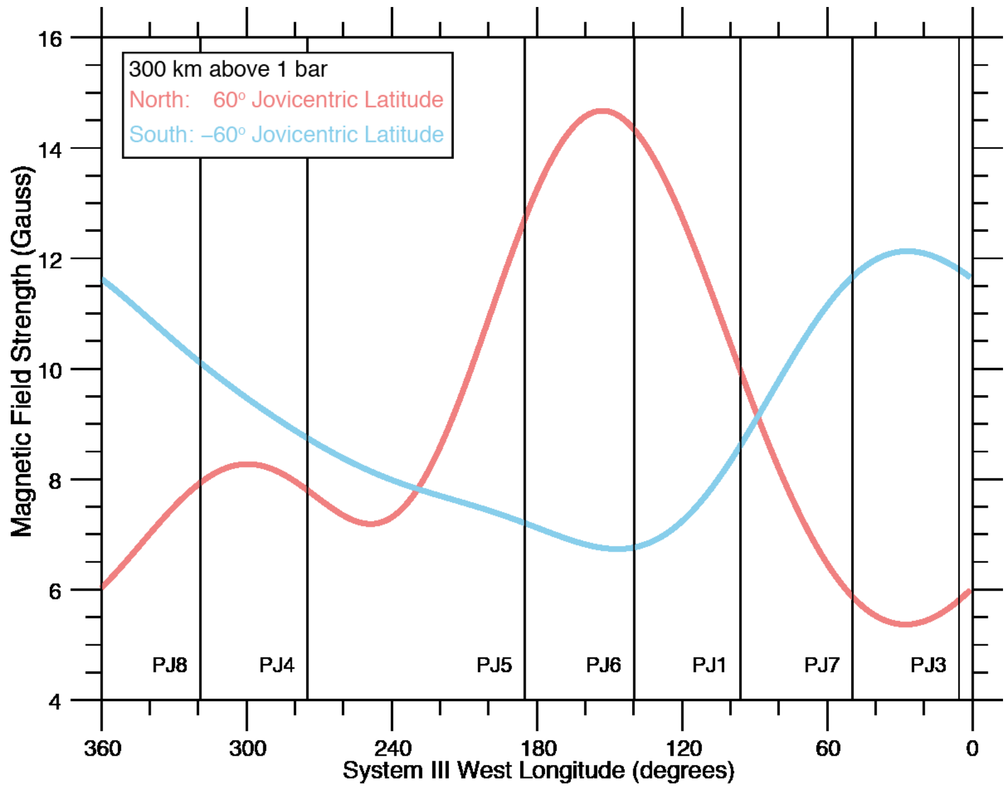

Supplementary Figure 9 | Magnetic field strength from the VIP4 model[18] as a function of longitude. The calculations are done at an altitude of 300 km above the 1 bar level for latitudes of +60° in the Northern hemisphere (red) and −60° in the Southern hemisphere (blue). Longitudes of the closest approaches to Jupiter for separate Juno orbits (PJ1-PJ8) are shown on the bottom. The case from Figure 1a belongs to the orbital segment PJ4, while the case from Figure 1b belongs to PJ6. Higher ionospheric magnetic fields in the northern hemisphere for PJ5 and PJ6 may in part explain the observed absence of more dispersed (class 2) events during these orbital segments, while for PJ7 and PJ8 we observe them also at higher positive latitudes (see Supplementary Figure 8). However, according to our analysis shown in Figure 4, lower ionospheric densities would also be necessary to explain the presence low dispersion (class 1) events.

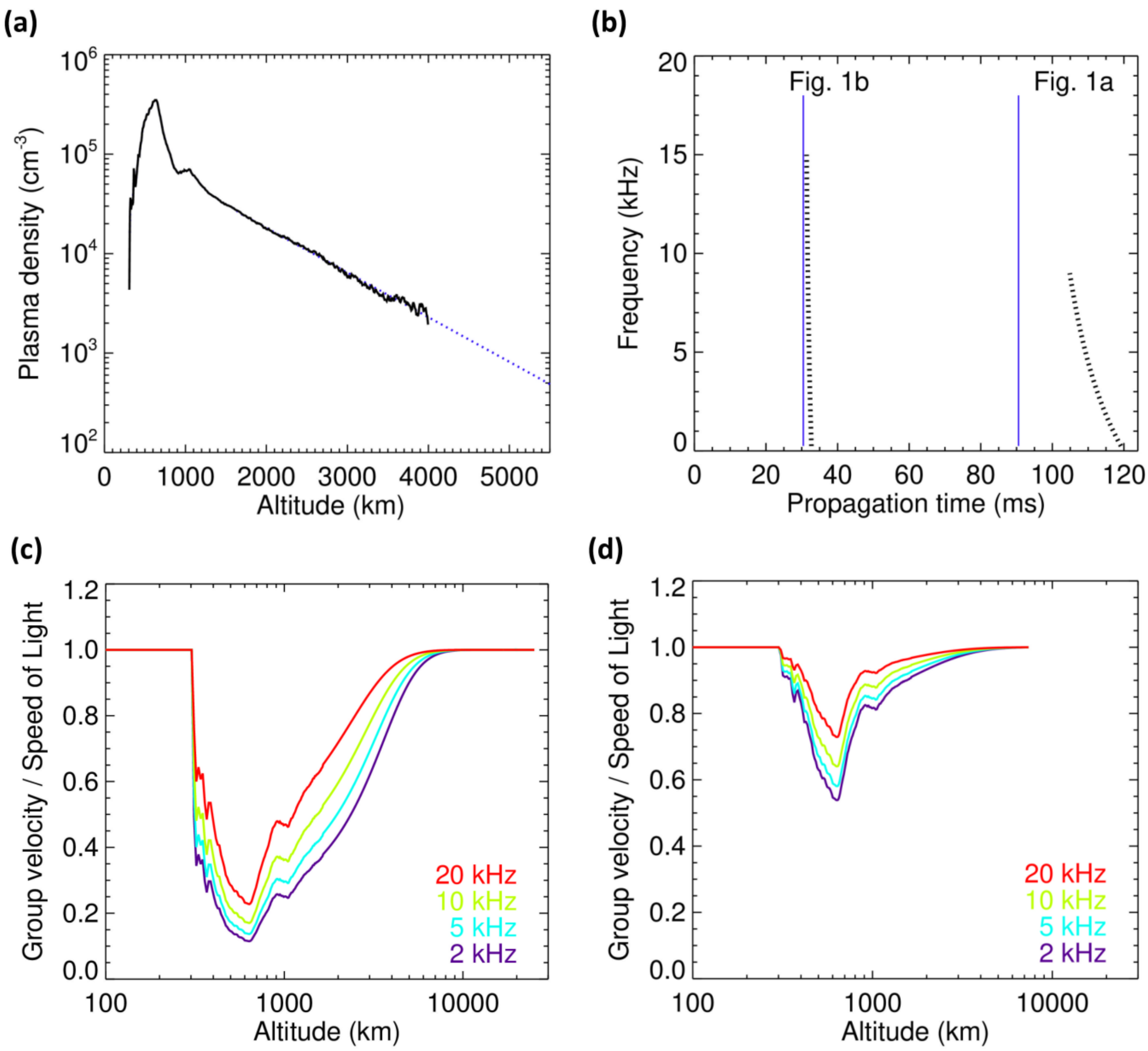

Supplementary Figure 10 | Calculations of the frequency dependent propagation delay shown in Fig. 1. (a) Solid line: Jovian ionospheric plasma density model from the Voyager 2 entry radio occultation[29] as a function of altitude *h*; blue dotted line: exponential extension of this model (Equation 7) which is used for altitudes above 1640 km. (b) Dotted lines: modelled field-aligned propagation time of Jovian rapid whistlers from Fig 1 starting from a pulse at zero altitude (1 bar level) below the Jovian ionosphere; vertical blue solid lines: speed of light propagation time. (c) Profiles of the group velocity calculated at 4 selected frequencies for the case in Fig 1a; (d) modelled group velocity profiles for the case in Fig. 1b for which the density model has been reduced by one order of magnitude and for which the rescaled magnetic field model (Equation 6) gives almost twice larger field strength compared to the event from Fig. 1a.

Supplementary Audio Guide- Sounds of Jovian lightning

Supplementary audio 1: Sound of whistler from Fig 1a

Supplementary audio 2: Sound of whistler from Fig 1b

Guide: Sound files containing waveforms for Jovian rapid whistlers shown in Fig 1. Left channel: electric field; right channel: magnetic field. The sampling frequency has been reduced by a factor of 10, in order to make the whistlers audible for all ages. The duration of each sound file is only slightly more than 1 second, so playing it in a "repeat" mode might be better for enjoying the acoustic beauty of Jovian lightning.

Supplementary Table 1 | Description of Supplementary data 1 – List of historical optical lightning detections

Each line in the data file *Supplementary_data_1.csv* represents one optical lightning detection reported in literature. Each line is composed of 6 items separated by commas.

1. Planetocentric latitude (°)
2. System III west longitude (°)
3. Mission (V1 – Voyager 1; V2 – Voyager 2; G – Galileo; C – Cassini; NH – New Horizons)
4. Source publication number from the list of references in the main paper
5. Method of data collection: TT – coordinates "taken from the text of the source publication"; MD – coordinates "manually digitized from a figure in the source publication"
6. Transformation from planetographic to planetocentric coordinates: Y- done, N-not needed

The data file contains 149 lines; the first ten lines are shown here:

Planetocentric latitude (deg)	Syst. III west longitude (deg)	Mission	Reference	Method of data collection	Coordinate Transformation
44.364	47.6	V1	16	TT	Y
45.17	48	V1	16	TT	Y
44.968	47.4	V1	16	TT	Y
43.962	45.4	V1	16	TT	Y
44.364	36	V1	16	TT	Y
43.36	34.6	V1	16	TT	Y
43.761	34.8	V1	16	TT	Y
45.372	36.8	V1	16	TT	Y
46.385	34.8	V1	16	TT	Y
44.968	33.6	V1	16	TT	Y

Supplementary Table 2 | Description of Supplementary data 2 – List of whistlers observed by Juno

Each line in the data file *Supplementary_data_2.csv* represents one snapshot during which Waves instrument onboard Juno detected one or more whistlers. Each line is composed of 6 items separated by commas.

1. Start of the snapshot (UTC: YYYY-MM-DD**T**HH:MM:SS.XXXXXX)
2. End of the snapshot (UTC: YYYY-MM-DD**T**HH:MM:SS.XXXXXX)
3. Juno System III west longitude (°)
4. Juno planetocentric latitude (°)
5. Juno radial distance in Jovian equatorial radii (71492 km)
6. Juno altitude (km) above the 1 bar surface calculated as a difference of radial distances for a given Juno latitude, with an oblate spheroidal model of the 1 bar surface having a polar axis of 66854 km and an equatorial axis of 71492 km.

The data file contains 1311 lines; the first ten lines are shown here:

Start of the snapshot (UTC)	End of the snapshot (UTC)	Juno west longitude (deg)	Juno planeto-centric latitude (deg)	Juno radial distance (RJ)	Juno altitude above 1bar level (km)
2016-08-27T12:29:42.770000	2016-08-27T12:29:42.892880	276.758	52.35	1.2696	22289
2016-08-27T12:29:50.770000	2016-08-27T12:29:50.892880	276.678	52.108	1.2672	22100
2016-08-27T12:29:54.770000	2016-08-27T12:29:54.892880	276.639	51.987	1.266	22006
2016-08-27T12:30:10.770000	2016-08-27T12:30:10.892880	276.481	51.498	1.2613	21630
2016-08-27T12:30:18.770000	2016-08-27T12:30:18.892880	276.402	51.253	1.2589	21443
2016-08-27T12:30:20.770000	2016-08-27T12:30:20.892880	276.382	51.191	1.2583	21396
2016-08-27T12:30:22.770000	2016-08-27T12:30:22.892880	276.362	51.13	1.2578	21349
2016-08-27T12:30:24.795000	2016-08-27T12:30:24.917880	276.342	51.067	1.2572	21302
2016-08-27T12:30:28.770000	2016-08-27T12:30:28.892880	276.303	50.945	1.256	21209
2016-08-27T12:30:52.770000	2016-08-27T12:30:52.892880	276.066	50.199	1.249	20653